

MONTE CARLO ANALYSIS ON NEUTRON SKYSHINE

T. Nakamura and T. Kosako*

Institute for Nuclear Study, University of Tokyo

This work systematically investigated, by Monte Carlo calculations, the skyshine of neutrons from monoenergetic neutron sources between 14 MeV and thermal energy fixed on the ground. The multi-group Monte Carlo code MMCR was developed for this study¹⁾ and the neutron skyshine in the air-over-ground environment up to about 2 km from a source has been calculated by including the ground effect on the transport in the air by the albedo method.

For a point isotropic source that emits one neutron within a cone having a half-apex angle of $\theta_s = 0, 30, 60$ or 85 deg, the calculated neutron energy spectrum becomes softer with increasing distance between the detector points and the source, and approaches an approximate equilibrium spectrum with near $1/E$ dependence in the keV region beyond about a few hundred meters from the source. Fig. 1 shows the variation of product of the detector distance and the dose equivalent $rD(r)$ with r for a source of $\theta_s = 0$. This figure clearly shows that the dose curves are well fitted by the following simple formula,

$$D(r) = \frac{Q_D(g_s, \theta_s)}{r} \exp\left(-\frac{r}{\lambda_D(g_s, \theta_s)}\right) \quad (1)$$

Two parameters, Q_D and λ_D , determined by least-square fittings of the calculated results in Fig. 1 are listed in Table I for each source energy group g_s and source opening angle θ_s . This simple formula is very useful, since one can easily estimate the skyshine neutron dose distribution by superposing Eq. (1) as

$$D(r) = \sum_{g_s} \frac{Q_D(g_s, \theta_s)}{r} \exp\left(-\frac{r}{\lambda_D(g_s, \theta_s)}\right) \phi_{g_s} \quad (2)$$

by knowing only the grouped source neutron spectrum ϕ_{g_s} .

The dose distributions and the energy spectra of neutrons have been measured with various detectors in the environment surrounding the electron synchrotron of the Institute for Nuclear Study, University of Tokyo, when the synchrotron were operated in the state of 650-MeV electron acceleration and about 10^{12} electrons/sec intensity. Almost all of the electrons were dispersed into the iron yoke magnet on the last stage of acceleration and generated neutrons by the $Fe(\gamma, Xn)$ reaction caused by photons from the electromagnetic cascade shower. This source neutron spectrum was approximated to be a synthesis of the Maxwellian spectrum and $E^{-\alpha}$ (E =neutron energy), as shown in Fig. 2. The synchrotron is covered with the concrete shield of 1-m-thick side wall and 0.5-m-thick ceiling. The neutron spectrum on the upper concrete shield was calculated by the two-dimensional discrete ordinate transport code, DOT3.5, and is shown in Fig. 2. This neutron spectrum becomes the skyshine source spectrum, since the dose level measured on the upper shield was about

5 to 10 times higher than that on the side wall.

The neutron dose in the field $D(r)$ was measured with a rem counter and a moderated big BF_3 counter as a function of the distance, r , from the center of the synchrotron ring²). By using the skyshine source spectrum in Fig. 2, the neutron dose was calculated by the MMCR code. Fig. 3 shows the comparison between calculated and measured dose distributions $rD(r)$. This relative comparison reveals the good agreement between calculation and experiment up to 600 m and the normalization factor of calculation to experiment corresponding to the absolute value of skyshine source strength is in good agreement with the average value measured on the upper shield.

*Present address: Research Center for Nuclear Science and Technology University of Tokyo

References

- 1) T. Nakamura and T. Kosako, Nucl. Sci. Eng., 77, 168 (1981).
- 2) T. Nakamura et al., Nucl. Sci. Eng., 77, 182 (1981).

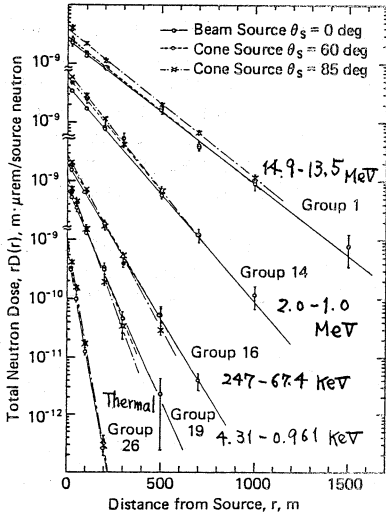


Fig. 1

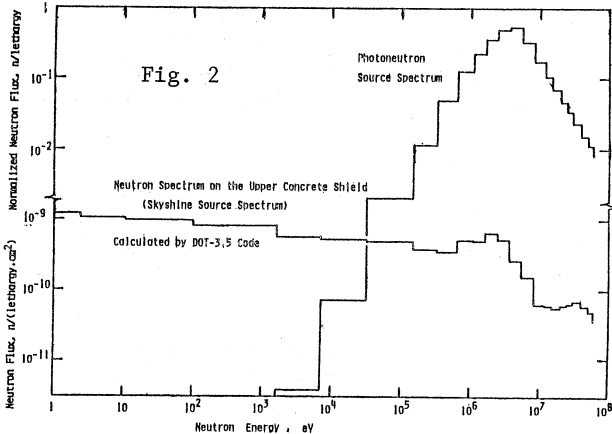


Fig. 2

Table I Estimated values of Q_D, λ_D^{-1}

Energy Group Number	$Q_D, \text{m} \cdot \mu\text{rem}/(\text{source neutron})$		
	Source Aperture Angle, θ_s (deg)		
	0	60	85
1	$2.52 \pm 0.21-9$	$2.90 \pm 0.17-9$	$3.82 \pm 0.15-9$
14	$3.99 \pm 0.16-9$	$5.49 \pm 0.70-9$	$7.40 \pm 0.07-9$
16	$2.11 \pm 0.03-9$	$2.50 \pm 0.15-9$	$2.93 \pm 0.12-9$
19	$8.18 \pm 0.28-10$	$1.02 \pm 0.06-9$	$1.25 \pm 0.06-9$
26	$8.06 \pm 0.46-10$	$8.90 \pm 0.31-10$	$1.21 \pm 0.05-9$
	$\lambda_D^{-1} (\text{m}^{-1})$		
1	$5.80 \pm 0.18-3$	$5.88 \pm 0.16-3$	$5.81 \pm 0.10-3$
14	$8.44 \pm 0.25-3$	$8.93 \pm 0.50-3$	$9.42 \pm 0.05-3$
16	$1.20 \pm 0.01-2$	$1.34 \pm 0.04-2$	$1.38 \pm 0.04-2$
19	$1.72 \pm 0.04-2$	$1.83 \pm 0.06-2$	$2.08 \pm 0.04-2$
26	$4.09 \pm 0.09-2$	$3.95 \pm 0.07-2$	$4.19 \pm 0.06-2$

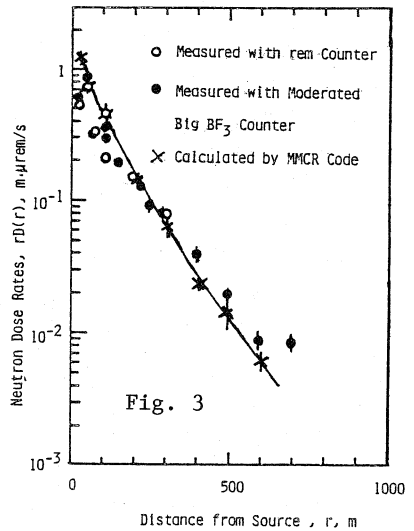


Fig. 3